Article

Monoclinic zirconium oxide nanostructures having tunable band gap synthesized under extremely non-equilibrium plasma conditions

Onkar Mangla[1] and Savita Roy[1,*]

[1] Physics Department, Daulat Ram College, University of Delhi, Delhi-110007, India; onkarmangla@gmail.com; savitaroy64@gmail.com

* Correspondence: savitaroy64@gmail.com; Tel.: +91-9810629598

Academic Editor: name

Received: date; Accepted: date; Published: date

Abstract: Zirconium oxide (ZrO_2) being a wide and direct band gap semiconductor used for fabrication of optoelectronic devices. ZrO_2 based optoelectronic devices span wide optical range depending on the band gap of ZrO_2 material. The band gap of ZrO_2 can be tuned by fabricating it to nanoscale. In this paper, we synthesized the ZrO_2 nanostructures on quartz substrate using ZrO_2 ions produced by the ablation of ZrO_2 pellet due to high temperature, high density and extremely non-equilibrium argon plasma in a modified dense plasma focus device. Uniformly distributed monoclinic ZrO_2 nanostructures of average dimension ~ 14 nm have been obtained as found from X-ray diffraction and Scanning electron microscopy studies. The monoclinic phase of ZrO_2 nanostructures is further confirmed from photoluminescence (PL) and Raman spectra. PL spectra show peaks in ultra-violet (UV), near-UV and visible regions with tunable band gap of nanostructures. Similar tunability of band gap has been observed from absorption spectra. The obtained structural, morphological and optical properties are correlated to investigate the potential applications of ZrO_2 nanostructures in optoelectronic devices.

Keywords: Nanocrystalline materials; Zirconium oxide; Synthesis; Luminescence; Energy band gap.

1. Introduction

Zirconium oxide (ZrO_2) is an interesting semiconducting material having wide band gap, which is being studied extensively to explore its fundamental properties for making high efficient devices. The band gap of ZrO_2 decreases on increasing the processing temperature, which makes it more conductive and hence it can be used in applications-oriented research. ZrO_2 has high melting point, high mechanical and thermal resistance, high dielectric constant and low electrical conductivity. ZrO_2 is also chemically stable with excellent hardness and biocompatibility, which render it as a suitable candidate to be used for chemical, optical, dielectric and mechanical applications [1-3]. ZrO_2 has potential to be used in making fuel cells [4], protective coatings for mirrors [3] and optoelectronic devices [5]. ZrO_2 possess high dielectric constant, which makes it an ideal candidate for replacement of conventional gate oxide in field effect transistors in the future generation nanoelectronic devices.

The physical properties of the ZrO_2 are influenced significantly by its crystal structure. ZrO_2 exists in three polymorphic phases depending upon the growth temperature i.e. monoclinic (exists at low temperatures below 1150 °C and it is a thermodynamically stable phase), tetragonal (exists at intermediate temperatures within the range of 1150-2370 °C) and cubic (exists a very high

temperature greater than 2370 °C) [6]. The monoclinic crystal structure being the thermodynamically stable phase fulfills the stability requirement of ZrO_2 based nanoelectronic devices. ZrO_2 when fabricated at nanoscale results in emission peaks at short-wavelength typically in UV region, which have applications in making read heads of compact discs (CDs) and increasing storage density of CDs [7,8]. In addition, the band gap of ZrO_2 can be tuned at nanoscale which increases the applications and also the efficiency of fabricated devices.

ZrO_2 nanostructures have been fabricated in variety of morphologies such as nanoparticles [9], nanobars [10], nanobelts [11], nanowires [12] and nanotubes [13]. The fabrication of these different morphologies of ZrO_2 nanostructures are mainly by the chemical methods. However, the chemical methods have used several precursors and other reacting agents which ultimately induces the impurity in nanostructures making them unqualified for fabricating high efficient devices. Plasma-assisted methods overcome the disadvantages of the chemical methods in the fabrication of nanostructures. Moreover, the fabrication of ZrO_2 nanostructures using a plasma-assisted methods has not yet reported in the literature. Thus, it is necessary to study the properties of ZrO_2 nanostructures when fabricated using a plasma-assisted technique.

This paper reports the synthesis of ZrO_2 nanostructures on quartz substrate using the material ions produced due to the ablation of ZrO_2 pellet by the hot, dense and extremely non-equilibrium argon plasma generated in a modified dense plasma focus (DPF) device. The properties of ZrO_2 nanostructures such as morphological, structural and optical have been studied and discussed in comparison with the earlier reports.

2. Results and Discussion

Figure 1a shows the scanning electron microscopy (SEM) image of deposited sample, indicating formation of uniformly distributed ZrO_2 nanostructures having surface density ~ 4100 nanostructures/μm^2. The size distribution of ZrO_2 nanostructures is shown in inset of Figure 1a and the peak of Gaussian profile in histogram gives average dimension of nanostructures ~ 14 nm. Transmission electron microscopy (TEM) image shown in Figure 1b confirms the formation of nanostructures with morphology similar to that obtained in SEM results. However, it is difficult to estimate the size distribution from TEM image thus a typical nanostructure with dimension ~ 15 nm is shown by arrow in Figure 1b. The morphology and dimension of nanostructures obtained from TEM results is in good agreement with that obtained from SEM results.

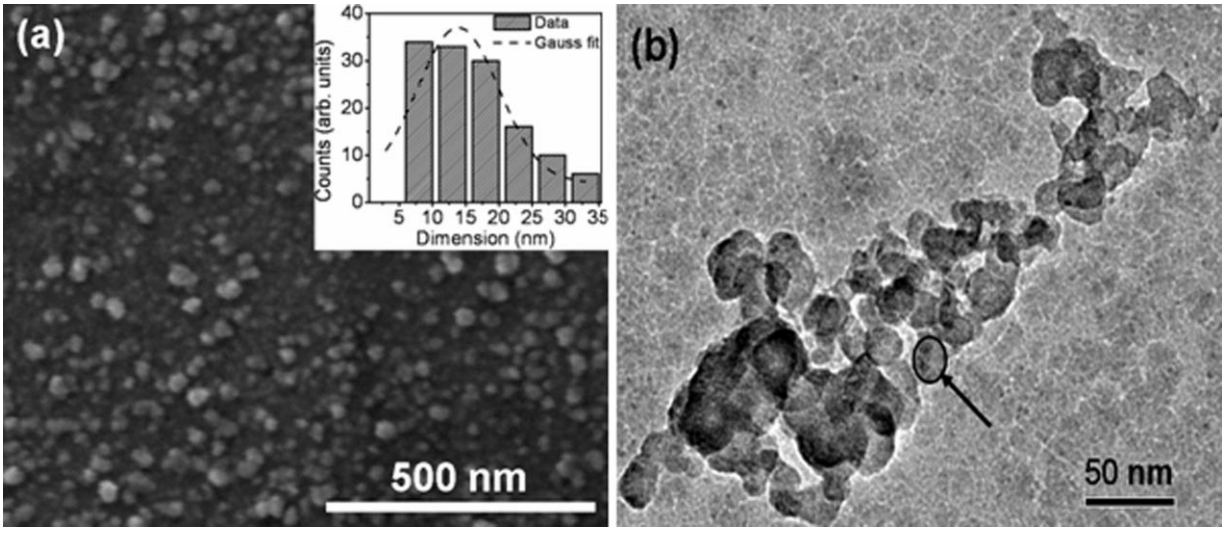

Figure 1. (a) SEM image (inset show size distribution) and (b) TEM image of ZrO_2 nanostructures.

In order to investigate the crystalline phase of ZrO_2 nanostructures, X-ray diffraction (XRD) studies have been carried out. XRD pattern shown in Figure 2 have crystalline diffraction peaks at 2θ values of 28.2°, 31.5°, 38.5°, 50.1° and 59.8° corresponding to [-111], [111], [120], [022] and [131] planes,

respectively of monoclinic ZrO_2 (ICDD File No. 37-1484). The grain dimension is found from Debye Scherrer's equation

$$D = \frac{0.9\lambda}{\beta \cos\theta}, \quad (1)$$

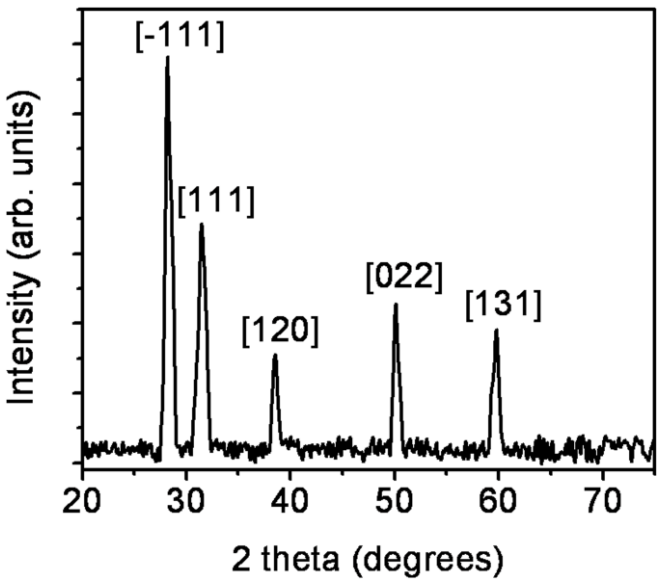

Figure 2. XRD pattern of ZrO_2 nanostructures.

where D is grain dimension in nm, λ is wavelength in nm, β is full width at half maxima (FWHM) in radians and θ is angle of diffraction corresponding to peak. The grain dimension has been found for each peak of XRD pattern individually and the average has been taken. The average grain dimension is found to be about 14 nm, which is in good agreement with the dimension of nanostructures obtained from SEM and TEM results. The length of dislocation per unit volume i.e. dislocation density (δ) depends upon grain dimension (D) as

$$\delta = \frac{1}{D^2}, \quad (2)$$

In addition, the strain (ε) produced in the film or nanostructures due to presence of such dislocations can be calculated using the relation

$$\varepsilon = \frac{\beta \cos\theta}{4}, \quad (3)$$

The obtained values of 2θ, θ, β, D, δ and ε have been summarized in Table 1. The average strain produced in nanostructures is ~ 2.5 x 10^{-3} indicating good quality of deposited nanostructures.

Table 1. Structural parameters of ZrO_2 nanostructures obtained from XRD pattern.

2θ (°)	θ (°)	β (radians)	D (nm)	δ (x 10^{-3} nm^{-2})	ε (x 10^{-3})
28.2	14.1	0.01166	12	6.94	2.83
31.5	15.75	0.01307	11	8.26	3.14
38.5	19.25	0.00865	17	3.46	2.04
50.1	25.05	0.00936	16	3.91	2.12
59.8	29.9	0.01089	15	4.44	2.36

The monoclinic structure of ZrO_2 nanostructures has been confirmed using photoluminescence (PL) and Raman spectra. The PL spectrum shown in Figure 3a has peaks at 376 nm (3.29 eV), 408 nm (3.04 eV) and 478 nm (2.59 eV). The peak obtained at 376 nm lies in UV region and it arises due to presence of oxygen vacancies in the nanostructures. These oxygen vacancies make the extrinsic states between valence band and conduction band yielding radiative transition at energy lower than band

gap of ZrO_2 (~ 5 eV). The decrease in energy of this radiative transition is also associated with the size and crystal quality of nanostructures which ultimately shift the emission spectra. Similar peaks near 376 nm have also been observed by several researchers [8, 14-16] for ZrO_2 nanostructures. In the present experiment, ZrO_2 get ionized into zirconium and oxygen ions which subsequently upon reaching the substrate recombine to form ZrO_2 nanostructures. However, in the process of recombination several oxygen-oxygen atoms recombine to form oxygen gas molecule which is lost from the material yielding oxygen vacancy in ZrO_2 nanostructures.

The PL peak at 408 nm lies in near-UV region and it arises due to transition from mid-gap trap state to valence band. The mid-gap trap states are formed mainly due to surface defects such as dislocations which are prominent in smaller dimension nanostructures. Similar peak has been observed in literature [14,17,18] by other researchers for ZrO_2 nanostructures. On the other hand, peak at 478 nm is characteristic peak of monoclinic ZrO_2 [19]. The monoclinic phase of ZrO_2 obtained in PL spectra is in confirmation with that obtained in XRD results. PL spectra reported in most of the earlier research papers [8, 14-16,18,19] consists only one broad band arise from defect states such as oxygen vacancies. The ZrO_2 nanostructures deposited in the present experiment using high fluence ions in modified DPF device have multiple peaks in PL spectra lying mainly in UV and near-UV regions. The observation of multiple peaks in PL spectra of nanostructures is due to tuning of band gap of ZrO_2 by the action of highly energetic and high fluence ions. This tuning of band gap and emission in UV, near-UV and visible regions render the deposited ZrO_2 nanostructures suitable candidate for optoelectronic device applications. Moreover, the use of plasma-assisted method such as modified DPF device results in multiple peaks in PL spectra, which render these ZrO_2 nanostructures to be used in wide optical range for fabrication of optoelectronic devices. On the other hand, in chemical methods the optical range of optoelectronic devices is narrow due to single broad band in PL spectra. This shows the clear advantages of plasma-assisted method i.e. modified DPF over chemical methods for making ZrO_2 nanostructures more viable to be used in device applications.

The monoclinic phase of ZrO_2 nanostructures obtained from PL and XRD results is further confirmed from Raman spectra. The Raman spectra shown in Figure 3b have peaks at 178, 189, 476 and 520 cm^{-1} which all are attributed to monoclinic phase of ZrO_2 [15,18,20].

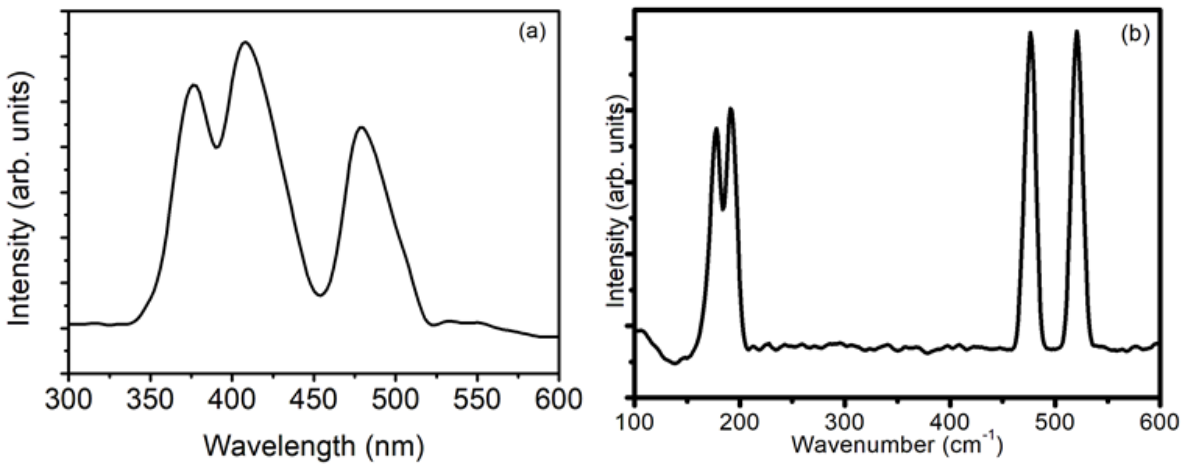

Figure 3. (a) PL spectra and (b) Raman spectra of ZrO_2 nanostructures.

The band gap of nanostructures has been tuned as obtained from PL results and to ascertain the value of band gap, absorption spectra has been taken which is shown in Figure 4a. It shows a peak at 292 nm which arise due to transition from valence band to conduction band [8,14,18]. As the ZrO_2 nanostructures have monoclinic structure thus the transition involved in this peak is mainly due to Zr^{3+} ions in the interstitial [21]. Tauc plot given in Figure 4b gave the band gap of nanostructures ~ 2.67 eV. Hence the ZrO_2 nanostructures have tuned band gap which lies in the region of observed PL peaks. The tunability of band gap also suggests possible applications of nanostructures in enhancement of solar cell efficiency.

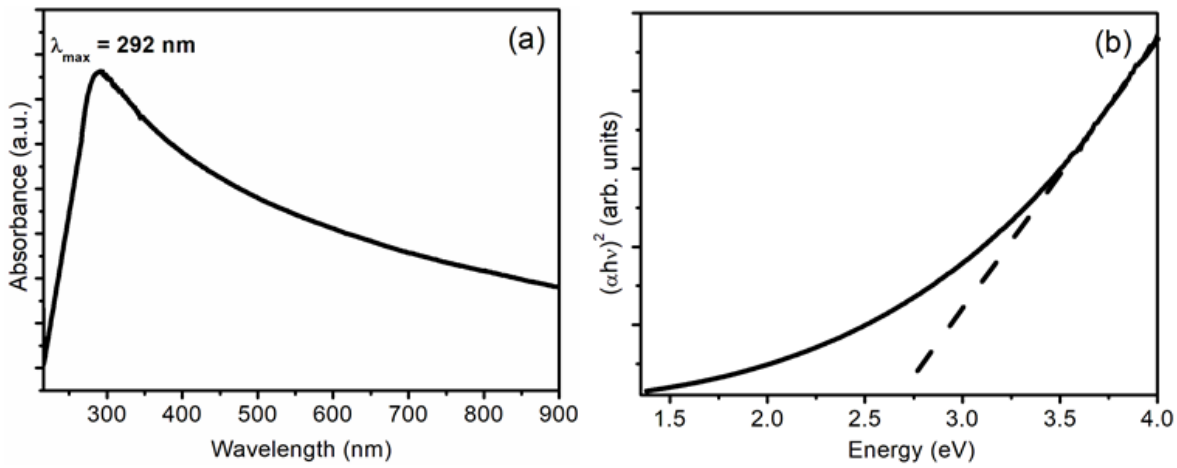

Figure 4. (a) Absorption spectra and (b) Tauc plot of ZrO_2 nanostructures.

3. Materials and Methods

ZrO_2 nanostructures were synthesized on quartz substrate in the modified DPF device. The target used for deposition was ZrO_2 pellet, which was made using ZrO_2 powder (99.99% pure) by compressing it to a pressure of 10 MPa and subsequently sintered them at a temperature of 800 °C for 6 hours. The quartz substrates were cleaned ultrasonically and were placed at an optimum distance of 5.0 cm from anode top. Two bursts of focused plasma were used for deposition of ZrO_2 nanostructures. The process of formation of high temperature, high density and extremely non-equilibrium argon plasma on the top of anode along with the modifications to DPF device for nanofabrication have been reported in earlier literature [22,23]. The focused argon plasma formed at top of modified anode ablates ZrO_2 pellet and ablated material ions move vertically upward in fountain like structure and get deposited on quartz substrates. The obtained samples were analyzed to study their morphological, structural and optical properties using different characterization techniques. The surface morphology was studied using SEM and TEM on Environmental scanning electron microscope model Quanta 200 FEI and transmission electron microscope model FEI G^2 Tecnai, respectively. Structural properties were studied using XRD pattern taken on D8 DISCOVER X-ray diffractometer having Cu Kα radiation of wavelength 1.54 Å. The room-temperature PL was done on Fluorolog (HORIBA JOBIN-YVON) spectrofluorophotometer using 270 nm (4.59 eV) excitation wavelength from a xenon flash lamp. Raman spectra were measured on in-Via Reflex (Renishaw) spectrometer equipped with Ar-Ne laser. Absorption spectra were taken on Perkin Elmer Lambda 35 ultra violet-visible (UV-VIS) spectrophotometer in absorption mode.

4. Conclusions

ZrO_2 nanostructures have been fabricated using material ions in the modified DPF device. The nanostructures have uniform distribution with average dimension of ~ 14 nm. ZrO_2 nanostructures have monoclinic phase, possess nanograins and have low strain obtained from XRD pattern. UV and near-UV peaks are obtained in PL spectra due to defects and dislocations. PL and Raman spectra confirm the monoclinic phase of ZrO_2 nanostructures. ZrO_2 nanostructures have tunable band gap obtained from PL and absorption studies. The optical band gap so obtained from PL and absorption spectra suggest possible applications of nanostructures in optoelectronic devices and efficiency enhancement of solar cells.

Acknowledgments: Authors are thankful to the University Science Instrumentation Center (USIC), Delhi University for providing characterization facilities.

Author Contributions: Both the authors conducted the study, analyzed the data and drafted the manuscript. Both the authors approved the final version.

Conflicts of Interest: The authors declare no conflict of interest.

References

1. Garvie, R.C.; Hannink, R.H.; Pascoe, R.T. Ceramic steel. *Nature* **1975**, 258, 703-704.
2. Wilk, G.D.; Wallace, R.M.; Anthony, J.M. High-κ gate dielectrics: Current status and materials properties considerations. *J. Appl. Phys.* **2001**, 89, 5243-5275.
3. Zhang, Q.; Shen, J.; Wang, J.; Wu, G.; Chen, L. Sol–gel derived ZrO_2–SiO_2 highly reflective coatings. *Int. J. Inorg. Mater.* **2000**, 2, 319-323.
4. Koch, T.; Ziemann, P. Zr-silicide formation during the epitaxial growth of Y-stabilized zirconia films on Si(100) and its avoidance by ion beam assisted deposition at a reduced temperature. *Appl. Surf. Sci.* **1996**, 99, 51-57.
5. Wang, X. ; Zhai, B. ; Yang, M .; Han, W. ; Shao, X. ZrO_2/CeO_2 nanocomposite: Two step synthesis, microstructure, and visible-light photocatalytic activity. *Mater. Lett.* **2013**, 112, 90-93.
6. Gao, P.; Meng, L.J.; dos Santos, M.P.; Teixeira, V.; Andritschky, M. Study of ZrO_2–Y_2O_3 films prepared by rf magnetron reactive sputtering. *Thin Solid Films* **2000**, 377, 32-36.
7. Huang, M.H.; Mao, S.; Feick, H.; Yan, H.; Wu, Y.; Weber, E.; Russo, R.; Yang, P. Room-temperature ultraviolet nanowire nanolasers. *Science* **2001**, 292, 1897-1899.
8. Cao, H.Q.; Qiu, X.Q.; Luo, B.; Liang, Y.; Zhang, Y.H..; Tan, R.Q.; Zhao, M.J.; Zhu, Q.M. Synthesis and Room-Temperature Ultraviolet Photoluminescence Properties of Zirconia Nanowires. *Adv. Funct. Mater.* **2004**, 14, 243-246.
9. Dwivedi, R.; Maurya, A.; Verma, A.; Prasad, R.; Bartwal, K.S. Microwave assisted sol–gel synthesis of tetragonal zirconia nanoparticles. *J. Alloys Compd.* **2011**, 509, 6848-6851.
10. Espinoza-Gonzalez, R.A.; Diaz-Droguett, D.E.; Avila, J.I.; Gonzalez-Fuentes, C.A.; Fuenzalida, V.M. Hydrothermal growth of zirconia nanobars on zirconium oxide. *Mater. Lett.* **2011**, 65, 2121–2123.
11. Jiang, C.; Wang, F.; Wu, N.; Liu, X. Up- and Down-Conversion Cubic Zirconia and Hafnia Nanobelts. *Adv. Mater.* **2008**, 20, 4826–4829.
12. Dong, W.-S.; Lin, F.-Q.; Liu, C.-L.; Li, M.-Y. Synthesis of ZrO_2 nanowires by ionic-liquid route. *J. Colloid Interface Sci.* **2009**, 333, 734–740.
13. Zhao, J.; Wang, X.; Zhang, L.; Hou, X.; Li, Y.; Tang, C. Degradation of methyl orange through synergistic effect of zirconia nanotubes and ultrasonic wave. *J. Hazard. Mater.* **2011**, 188, 231–234.
14. Kumari, L.; Li, W.Z.; Xu, J.M.; Leblanc, R.M.; Wang, D.Z.; Li, Y.; Guo, H.; Zhang, J. Controlled Hydrothermal Synthesis of Zirconium Oxide Nanostructures and Their Optical Properties. *Cryst. Growth Des.* **2009**, 9, 3874-3880.
15. Ling, X.; Li, S.; Zhou, M.; Liu, X.; Zhao, Y.; Shao, J.; Fan, Z. Annealing effect on the laser-induced damage resistance of ZrO_2 films in vacuum. *Appl. Opt.* **2009**, 48, 5459-5463.
16. Salavati-Niasari, M.; Dadkhan, M.; Davar, F. Pure cubic ZrO_2 nanoparticles by thermolysis of a new precursor. *Polyhedron* **2009**, 28, 3005-3009.
17. Liang, J.; Deng, Z.; Jiang, X.; Li, F.; Li, Y. Photoluminescence of Tetragonal ZrO2 Nanoparticles Synthesized by Microwave Irradiation. *Inorg. Chem.* **2002**, 41, 3602-3604.
18. Kumari, L.; Du, G.H.; Li, W.Z.; Vennila, R.S.; Saxena, S.K.; Wang, D.Z. Synthesis, microstructure and optical characterization of zirconium oxide nanostructures. *Ceram. Int.* **2009**, 35, 2401-2408.
19. Lai, L.-J.; Lu, H.-C.; Chen, H.-K.; Cheng, B.-M.; Lin, M.-I.; Chu, T.-C. Photoluminescence of zirconia films with VUV excitation. *J. Elect. Spectrosc. Relat. Phenom.* **2005**, 144-147, 865-868.
20. Kumari, L.; Li, W.Z.; Wang, D.Z. Monoclinic zirconium oxide nanostructures synthesized by a hydrothermal route. *Nanotechnol.* **2008**, 19, 195602 (7 pp).
21. Mikhailov, M.M.; Verevkin, A.C. The Variation of Band Gap Width in Zirconium Oxide Powders on Grinding. *Russ. Phys. J.* **2004**, 47, 600-604.
22. Mangla, O.; Srivastava, M.P. GaN nanostructures by hot dense and extremely non-equilibrium plasma and their characterizations. *J. Mater. Sci.* **2013**, 48, 304-310.
23. Mangla, O.; Roy, S.; Ostrikov, K. Dense Plasma Focus-Based Nanofabrication of III–V Semiconductors: Unique Features and Recent Advances. *Nanomater.* **2016**, 6, 4 (13 pp).